

Assessing urban population exposure risk to extreme heat: Patterns, trends, and implications for climate resilience in China (2000–2020)

Chengcong Wang ^{a,c}, Zhibin Ren ^{a,b,c,*}, Yujie Guo ^{a,c}, Peng Zhang ^{a,c}, Shengyang Hong ^{a,d}, Zijun Ma ^{a,c}, Wenhui Hong ^{a,c}, Xinyu Wang ^{a,c}

^a Key Laboratory of Wetland Ecology and Environment, Northeast Institute of Geography and Agroecology, Chinese Academy of Sciences, Changchun 130102, China

^b Key Laboratory of Tropical Island Land Surface Processes and Environmental Changes of Hainan Province, Haikou 571158, China

^c University of Chinese Academy of Sciences, Beijing 100049, China

^d Jilin Normal University, Siping 134000, China



ARTICLE INFO

Keywords:

Urban extreme heat exposure risks (UEHER)

Population exposed to extreme heat

Heat and health

Urban vulnerability

Spatio-temporal heterogeneity

ABSTRACT

Urban residents face serious thermal health risks from extreme heat owing to the cumulative effects of urbanization and climate warming. However, the patterns of urban populations exposed to extreme heat and urban extreme heat exposure risks (UEHER) require clarification in China. We determined urban extreme heat and the exposed populations for land surface temperature (LST) in 320 cities from 2000 to 2020 by setting thresholds and assessed the UEHER in China through the “Hazard-Exposure-Vulnerability” framework. Our findings indicated an average extreme LST threshold of 35.24 °C, varying from 29.32 °C to 47.79 °C. Higher extreme LST thresholds were mainly concentrated in Northwest China and developed cities. From 2000 to 2020, the extreme heat-exposed areas have increased by approximately 27.8 km², equivalent to an average of approximately 321.3 soccer fields per year. The urban population exposed to extreme heat (UPEEH) in China has increased by approximately 115 million in the past 20 years, mainly in more developed cities, especially in eastern and northern China. Notably, the proportion of the UPEEH has decreased more rapidly in the east region. The UEHER index increased 52.5 % over 20 years, with 97.19 % of the cities having a worsening trend. Medium-developed and high-population density regions faced the dual risk of a high UEHER and more rapid increase in extreme heat. In contrast, less-developed regions faced the dual problems of high UEHER and low gross domestic product (GDP). Understanding vulnerable and prioritized areas of urban heat exposure will provide information for the development of adaptive policies that enhance urban climate resilience.

1. Introduction

Global warming has escalated into a significant human concern (Chen et al., 2022b). In recent decades, global temperatures have been rising at a rate of 0.2 °C per decade and will likely increase more rapidly with time (Estoque et al., 2020; Lan et al., 2023). The effects on urban dwellers will be amplified by urban heat islands (UHI), which will cause urban heat waves and associated health risks. These are also expected to intensify in the coming years (Wang et al., 2021). The UHI is a major cause of urban extreme heat exposure (UEHE) (Tian et al., 2021; Wang et al., 2021). Wang et al. (2019) estimated that when the temperature rises by 1.5–2 degrees Celsius, the number of heat-related deaths among urban residents in China will exceed 279,000 per year.. In the context of

rapid urbanization (Ouyang et al., 2022), the convenience of urbanization has caused more than half of the population to move from rural areas to cities. Cao et al. (2022) note that the urban population is estimated to reach 68 % by 2050, adding to the burden of urban population exposure. Given the increasing risk of extreme heat exposure, if a city lacks immediate regulations, it may face persistent and serious threats. Therefore, understanding the distribution of the extreme heat exposure across cities is imperative.

When we talk about extreme heat exposure in cities, most current studies typically use air temperature and LST to represent the thermal environment in cities. Air temperature usually refers to the temperature in the atmosphere, which is the heat of the air (Martilli et al., 2020; Oke et al., 2017). LST refers to the temperature of the land surface (Tian

* Corresponding author at: Key Laboratory of Wetland Ecology and Environment, Northeast Institute of Geography and Agroecology, Chinese Academy of Sciences, Changchun 130102, China.

E-mail address: renzhibin@iga.ac.cn (Z. Ren).

et al., 2021). Therefore, changes in both air temperature and LST can have a significant impact on our lives and environment (Ullah et al., 2022). While extreme heat is the amount of heat felt by the human body, and air temperature can directly reflect the comfort level of the human body. However, in order to research the temperature heterogeneity within a city and the areas exposed to extreme heat, weather stations usually only provide temperature data on a local scale, which makes it difficult to fully reflect the spatial variation of LST. In addition, most studies have shown that LST is significantly and positively correlated with air temperature, which can be an important data for studying extreme heat exposure (Ma et al., 2023). In addition, the heterogeneity of LST can vary considerably from region to region, which can provide accurate guidance for future studies on intra-urban planning measures. Therefore, the use of LST data to study urban extreme heat exposure is currently the mainstream research method.

The study of extreme heat exposure has become a global research topic. Previous studies have focused on UHI, LST, and air temperature exposure (Siddiqui et al., 2021), and some have shown that the growing problem of UHI poses an increasing challenge (Li et al., 2022; Li et al., 2020; Liu et al., 2021), where the main reason for the decline in urban thermal comfort is climate change. The results of Cheng et al. (2023b) and Ren et al. (2022) suggest that rapid urbanization contributes 10.9 %, and significant spatial heterogeneity exists between climate zones (Chen et al., 2021; Zhao et al., 2014; Zhou et al., 2018). Extreme heat is defined as a climate that experiences abnormally high temperatures, that is, temperatures that are well outside the range expected from long-term climate data (Li et al., 2022; Yuan et al., 2022), and Massaro et al. (2023) express in terms of extreme land surface temperatures (LST). Extreme heat threatens human health and disrupts ecosystems, causing resource shortages and reduced crop yields (Ullah et al., 2022). Research on extreme heat can contribute to a clearer understanding of the environment in which people live, leading to better policies. Most current studies have only investigated extreme LST thresholds for a single city or uniformly identified extreme LST thresholds for multiple cities (Chen et al., 2022a; Freychet et al., 2022; Li et al., 2022; Ullah et al., 2022). It is debatable whether there are differences in the extreme LST thresholds in different cities owing to their geographical location and level of development. Although urbanization is caused by human aggregation, the background temperature for diverse populations living in cities only poses a health risk once different thresholds are exceeded (i.e., beyond the physiological tolerance of the human body) (Tian et al., 2021). It is one-sided to consider only the UHI temperature to directly reflect the threat of the thermal environment to the population (Hu et al., 2019; Sadeghi et al., 2021), and it does not reflect the quality of life or number of people exposed to extreme heat. Few studies have explored the exposure of urban populations to extreme LST in cities, particularly in developing countries. In addition, the background environments of different regions can lead to some variability in the populations threatened by extreme heat; therefore, discussing the distributional characteristics of populations threatened by extreme heat in different urban categories can provide adaptive policy support for the development of cities.

Urban extreme heat exposure risk (UEHER) assessment is an important part of the adaptation planning process, allowing decision-makers to identify how, where, and what risks are faced and high-risk areas on which to focus. Given the different urbanization developments, heterogeneity of urban background climate, inequality of urban green facilities, unequal distribution of vulnerable people, and density variability of urban populations, there may be instances where the LST is the same, but the UEHER differs (Chen et al., 2023; Hsu et al., 2021; Sun et al., 2020). However, most studies have quantitatively overlooked the human living environment by merely considering the UHI effect and extreme heat (Massaro et al., 2023; Sadeghi et al., 2021; Siddiqui et al., 2021; Yuan et al., 2022; Zhao et al., 2014), thereby failing to depict the UEHER comprehensively. In the Fifth Assessment Report (AR5), the Intergovernmental Panel on Climate Change (IPCC)

(<https://www.ipcc.ch/>) described the importance of vulnerability and exposure in risk assessment (Estoque et al., 2020; Huang et al., 2023; Zhu & Yuan, 2023), proposing a framework for assessing hazard-exposure-sensitivity (Flöttum et al., 2016). In other words, the risk of extreme heat exposure in each city not only comes from climate change, but also from the social development and the governance processes of each city that have an impact on the risk level in that city (Hu et al., 2019). The results of risk assessments based on this framework have been proven to be reliable, and several studies have applied this framework to the exploration of heat exposure risk (Cheval et al., 2023; Estoque et al., 2020; Huang et al., 2023; Zhu & Yuan, 2023). Currently, most of the studies focus on UHI and the studies are on the whole city scale (Hu et al., 2019; Sadeghi et al., 2021; Yuan et al., 2022), but in the city, the temperature varies from one area to another, and there are areas of extreme heat and areas of comfort, while there is a relative lack of studies on areas of extreme heat in the city, and there is a need for further exploration of spatial and temporal heterogeneity of the risk of extreme heat to populations. However, relying solely on risk indices without considering the heterogeneous heat exposure risks among cities and temporal trends may lead to untimely and ineffective policy responses. Moreover, large-scale studies offer a comprehensive understanding of complex phenomena; however, research on large-scale UEHER in China is lacking. The AR6 noted that the vulnerability and exposure of many cities have created a lock-in effect that makes change difficult and costly, thus exacerbating current social inequalities (Ish-tiaque et al., 2022). Therefore, it is important to study regional heterogeneity, which is essential to ensure social equity and sustainable development.

China has undergone rapid urbanization in recent years and is the most populous country in the world. As far as we know, research on the assessment of heat exposure in cities is limited, and our study topic needs to be better explored in China, both in scope and methodological approach. This study combines remote sensing and statistical data. This study encompassed three key aspects: (1) exploring the regional heterogeneity of extreme LST thresholds in different cities; (2) revealing spatiotemporal changes in urban extreme heat exposure in China; and (3) proposing a UEHER index based on the “hazard-exposure-sensitivity” assessment framework and exploring spatial heterogeneity and changes in the UEHER, prioritizing response measures for cities with higher risks and lower response capacities. This study explores important strategies in risk management aimed at reducing the impacts of climate change and threats to humanity through adaptation and mitigation measures.

2. Methodology

2.1. Study area

China is expansive in latitude and longitude and has complex and diverse topography (Dou & Kuang, 2020), diverse climatic backgrounds, and economic conditions (Han et al., 2022). Most cities in China experience significantly higher temperatures between June and August (Liu et al., 2021). Our research focused primarily on cities with urban centers spanning an area larger than 1000 ha to ensure accurate and reliable observations rather than considering administrative boundaries. Urban boundaries consist of artificially impermeable and non-urban areas within cities (Dong et al., 2022). A total of 320 cities were included in this study to ensure a complete dataset for each city under observation (Table S1). In 2020, the total population of the studied cities was 31.43 % of the country's total population.

We used geographic region, gross domestic product (GDP), and population to classify cities (Fig. 1). According to the geographic area, cities can be divided into Northeast China (NEC), Northern China (NC), Northwestern China (NWC), Southwestern China (SWC), central-southern China (CSC), and Eastern China (EC) (Fang et al., 2016). These cities can be divided according to their GDP in 2020: (< 10

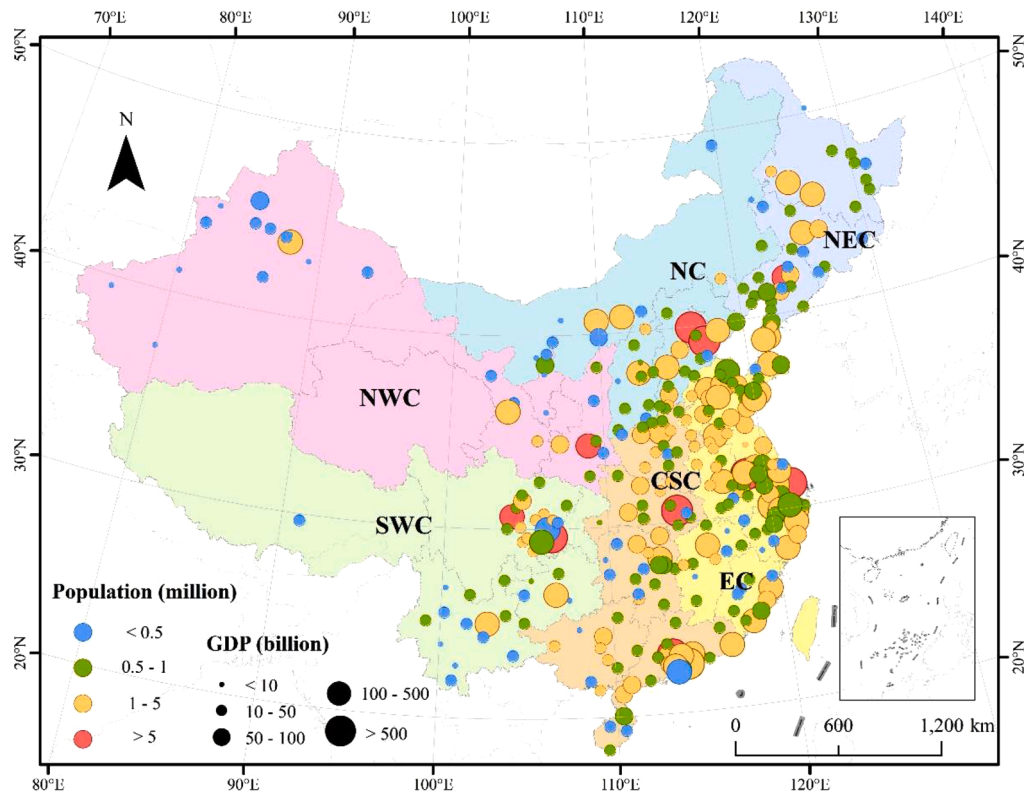


Fig. 1. Distribution and characteristics of the selected cities for this study. Note: map lines delineate study areas and do not necessarily depict accepted national boundaries

billion), (10–50 billion), (50–100 billion), (100–500 billion), and (> 500 billion). According to the population can be divided into (< 0.5 million), (0.5–1 million), (1–5 million), and (> 5 million) (Dong et al., 2022). By classifying Chinese cities at different levels, the patterns of cities at different levels can be accurately understood so that policymakers can plan according to city characteristics.

2.2. The conceptual framework for our study

We devised a conceptual framework by gathering LST data spanning 2000 – 2020 for 320 cities and considering insights from the existing literature alongside the discerned research gaps. First, we determined extreme Land Surface Temperature (LST) thresholds for each city. The results represented the differences in living environments across different cities. Next, we utilized the extreme LST threshold to calculate the number of people and trends in exposure to extreme heat in each city, the population exposed to extreme heat in our study was assumed to be exposed to the urban outdoor thermal environment. Based on this, we comprehensively assessed urban extreme heat exposure risks (UEHER) levels and trends in each city using the “Hazard-Exposure-Vulnerability” framework to provide prioritized corrective measures and necessary guidance for areas with higher risk and weaker coping capacities.

2.3. LST data acquisition and the indicators representing UEHE

The relationship between remotely sensed LST and air temperature measured by weather stations is complex, with a clear spatial regression. In the context of UHI studies, we can assume that the relationship between LST and air temperature shows a clear similarity, but air temperature cannot be expressed in terms of spatial distribution within cities (Cao et al., 2020; Li, 2021; Yuan et al., 2022). Therefore, the LST is a useful and plausible dataset that can be expressed in multiple

dimensions at spatial and temporal resolutions. Based on previous studies, we used a remotely sensed LST dataset to explore the urban extreme heat. The LST was obtained from the MOD11A1 V6.1 product provided by NASA, with a resolution of 1 km × 1 km, and daily LST was provided by MODIS. Converting MODIS pixel values to LST requires multiplying by 0.02 and subtracting 273.15. Because of the lower temperature at night compared to the daytime, we selected daytime data from the MODIS data for the study. Data from June to August were averaged to determine the summer daytime LST data for that year.

2.3.1. Urban extreme LST

The extreme LST threshold has no definitive value for each city, and the 90th percentile determination of the threshold has been widely used in previous studies (Chen et al., 2022a; Cheng et al., 2023a; Massaro et al., 2023). As shown in Fig. 2a, we define the urban extreme heat zone as the LST that exceeds the extreme LST threshold. For each city, the thresholds have been computed as the 90th percentile of the distribution of the LST over 20 years of observation (from 2000 to 2020) of all pixels of the city.

2.3.2. Urban population exposed to extreme heat (UPEEH)

When the LST in a certain region of a city exceeds the extreme LST thresholds, this region is defined as an extreme heat region of the city, and residents living there are at risk of extreme heat exposure (Sherwood & Huber, 2010). The UPEEH was defined as the sum of the number of people in an urban pixel cell whose LST exceeded the extreme LST threshold (Fig. 2b).

2.3.3. Extreme heat exposed areas

Urban heat-exposed areas can threaten residents who can sense urban heat waves but are unaware of specific heat-exposed areas. Therefore, identifying areas where LST exceeds extreme LST thresholds in each city can help us understand the areas of extreme heat in the city.

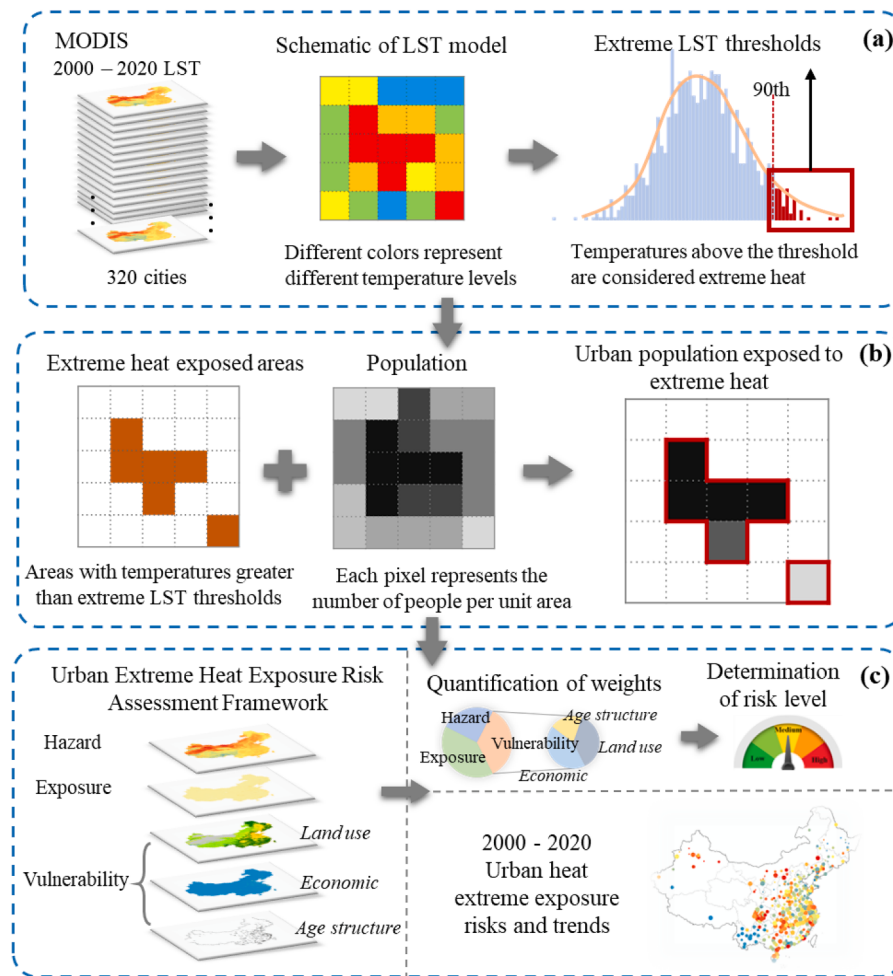


Fig. 2. Design and framework of the study. (a) Model diagram for LST acquisition and confirmation of extreme LST thresholds; (b) Schematic of the model to calculate the extreme heat-exposed population of the city; (c) Diagram showing the risk-assessment framework employed to operationalize the IPCC's risk concept in its AR5 and Assessment of urban extreme heat exposure risk and its trends

Urban heat-exposed areas were calculated using the equal-area projection method for pixel areas in which the LST for a city was greater than the sum of the extreme LST thresholds (Fig. 2b).

2.3.4. Years of continuous extreme heat exposure

In this study, we propose the years of continuous extreme heat exposure to explain the characteristics of consecutive extreme heat exposure in different cities in China; if the years of conscious extreme heat exposure in a city is higher, the more threatened the population in that city is by extreme heat. Therefore, we determine in advance whether a city has urban population exposed to extreme heat in order to determine whether the city is in an extreme heat-exposed year.

2.3.5. The percentage of urban population exposed to extreme heat

This indicator reflects the proportion of the people in a city facing the threat of extreme heat. The calculation method involved dividing the people exposed to extreme heat in a city in a given year by the total population of that city in the same year.

2.4. Quantification of weights and UEHER assessment

To determine weights, this study used hierarchical analysis as the main tool. The analytic hierarchy process (AHP) combines qualitative and quantitative weighting judgment methods for solving complex problems with multiple objectives. The AHP relies on expert judgment for moderate feedback throughout the process (Wu & Tang, 2022). Thus,

experts were drawn from professionally relevant practitioners (Cheval et al., 2023). These experts assessed the relative significance of the measures, assigned importance levels to the chosen indicators, and rationally assigned weights to each criterion for every decision option. They compared the significance of each indicator using importance level values ranging from 1 to 9 (Table S3) (Iaria & Susca, 2022).

A matrix is created for each expert's two-by-two comparison of rating values, the eigenvectors are obtained, and the maximum eigen root λ_{\max} of the matrix is calculated, and then the consistency index CI value is calculated as (Eq. 1)

$$CI = \frac{\lambda_{\max} - n}{n - 1} \quad (1)$$

A third-order matrix was constructed, corresponding to a random consistency value of RI = 0.52.

The formula for the consistency ratio CR value is (Eq. 2)

$$CR = \frac{CI}{RI} \quad (2)$$

In the AHP, a CR value below 0.1 (10 %) indicated reliability and consistency within the data. If the CR value surpasses 0.1, this implies an inconsistency. Among the 20 expert scoring sets collected, eight results that failed the consistency test were excluded. Consequently, the application of AHP in this survey is robust, free from biases in weighted judgment results, reliant on expert decisions, and ensures the internal consistency of expert outcomes.

Using a risk-assessment framework, we constructed a hazard-exposure-sensitivity assessment system (Estoque et al., 2020; O'Lenick et al., 2019). The UEHER index for each city was obtained by averaging the scoring results of the 12 experts and determining the weight values for each assessment factor. Our study integrated remote-sensing and socio-ecological data, aligned with the combined evaluation principle supported by most studies. This framework comprises three components: hazards, exposure, and vulnerability. Vulnerability encompasses economic status, age structure, and land use (Table S2), aggregating each indicator by relative weighting (Li et al., 2022).

To measure the UEHER index for each city, we normalized the indicator data to be in the range of 0-1 to make the indicators comparable. The normalization method we chose was max-min, using the same method for all indicators (Table S5) (Eq. 3).

$$RI_i = \sum_{j=1}^n x_{ij} w_j \quad (3)$$

The UEHER risk index RI_i for city i is a weighted sum of the framework components of the UEHER index, where x_{ij} is the value of index j in city i , and w_j is the relative weight of index j , where $n = 3$, representing hazard, exposure, and vulnerability, and the sum of the weights of these three components is 1. Based on the 12 sets of relative weights provided by expert scoring, each city produced 12 risk-assessment results (Table S4), which are 12. The average of these 12 results was the UEHER index of the city (Estoque et al., 2020). After deriving the UEHER index, we normalize the risk so that it is normalized to the 0-1 range, a scale that is not absolute but relative. The levels are categorized as: high (0.80 to 1.00), medium-high (0.60 to 0.80), medium (0.40 to 0.60), medium-low (0.20 to 0.40), and low (0.00 to 0.20) (Cheval et al., 2023; Estoque et al., 2020).

2.4.1. Heat hazard index

Previous studies have shown that LST remote-sensing data can be used as a representative heat indicator (Wang et al., 2022a; Wu & Tang, 2022; Yuan et al., 2022). Urban heat waves are most likely to occur during the summer months and pose significant heat-related health risks. In China, there is little north-south variation in summer temperatures, and although hot weather can happen in the south during spring and fall, this is still a relatively low heat risk compared with summer (Wang et al., 2023a). Thus, we focused on data from June to August, the hottest month between 2000 and 2020, to explore heat hazards. This provides an exploration of changes in the temporal and spatial dimensions. We extracted daily LST data from the MODIS product on the GEE platform, which contained both daytime and nighttime temperature values. In our study, we specifically considered daytime temperature data because of their association with higher heat risk indices. However, cloud cover was more prevalent during the summer, particularly in the southern region. To circumvent temperature value errors owing to cloud interference, we opted for the highest temperature every eight days as a representative temperature image during this period. This method yielded 11 images from June to August, then averaged to form the LST map for each year, spanning 21 years. With the city boundaries delineated, LST values surpassing the extreme LST threshold for each city were employed as heat hazard values. Subsequently, we normalized the heat hazard data to ensure that the values were scaled from 0 to 1, spatially and temporally.

2.4.2. Heat exposure index

We define exposure as one of the indicators. The population is affected by high temperatures, and population density is an indicator of UEHE. Population density is a better indicator of population concentration than the number of people in the city. For many years, WorldPop has provided population-gridded data products with a spatial resolution of approximately 1000 m (www.worldpop.org), where the population density dataset is obtained by dividing the number of people per pixel by

the surface area of that pixel. Many studies confirm the availability and veracity of these data (Dong et al., 2022; Wang et al., 2023a); that is, the regression curve between population density and total city population has a very strong positive correlation. We obtained the UEHER index for each city in terms of time and space for 320 cities from 2000 to 2020. Similar to the heat hazard index, we first extracted the mean population density for each city using city boundaries and normalized the temperature data for each city to a range of values from 0 to 1 on both temporal and spatial scales.

2.4.3. Heat vulnerability index

It is noted in AR6 that, since AR5, there is growing evidence of the importance of vulnerability in the UEHER. Vulnerability is a combination of a city's ability to cope with heat hazards and its ability to harm human health (Ishtiaque et al., 2022; O'Lenick et al., 2019). Considering the availability of data, we identified vulnerability factors for cities, including the economic level of the city, the ratio of impervious surface to green space, and the proportion of the population aged over 65 years. In addition, all data are temporal and spatial, except for the proportion of the population over 65 years of age, meaning that the values of these indicators could be calculated for each year according to city boundaries and normalized between 0 and 1 in time and space. At the economic level of a city, the ability to cope with heat hazards is inversely proportional to vulnerability; thus, the indicator is negative when calculating the urban vulnerability index. The economic level of each city was the sum of the city boundaries, pixel values, and GDP dataset provided by the Geographic Remote-Sensing Ecology Network Platform (www.gisrs.cn). The impervious area and green space ratios can reflect both green space and urbanization development; the higher the ratio, the lower the green space ratio, and the less it can balance the pressure caused by the urban thermal environment. Land-use data for this study were obtained from the National Land-Use Classification (<https://doi.org/10.5281/zenodo.5816591>). Elderly individuals are less physically active and more sensitive to heat. When a city has a higher proportion of elderly population, it is also has a higher risk of mortality. Data were obtained from the 5th (2000), 6th (2010), and 7th (2020) census sub-counties (<http://www.stats.gov.cn>). These were statistical data, and we queried the proportion of the population in each age group for the 320 study cities. Because these data were not continuous, we fitted the change curve as a percentage of the number of people over 65 years per year. The final vulnerability value for each city was determined based on the scoring weights of 12 experts and normalized to a range of 0-1 based on the time and spatial scales.

3. Results

3.1. Spatial distribution of urban extreme LST thresholds

The results showed significant spatial heterogeneity in extreme LST thresholds between different cities. The national mean extreme LST threshold was 35.24 °C (Fig. 3a), with a maximum of 47.79 °C and a minimum of 29.32 °C. The higher extreme LST thresholds were mainly concentrated in the NWC desert region with an average high extreme LST threshold of 38.09 ± 3.68 °C, 2.85 °C higher than the national average, followed by the NC (35.88 ± 1.65 °C), the CSC (35.52 ± 0.98 °C), and the EC (35.45 ± 0.91 °C). Conversely, the lower thresholds were evident in NEC at high latitudes (33.52 ± 1.41 °C) and SWC at high altitudes (33.03 ± 2.07 °C), both approximately 2.21 °C below the national average (Fig. 3b).

From a population and economic perspective, the more densely populated and economically developed the region, the higher the extreme LST thresholds. Notably, the extreme LST thresholds are about 1 °C higher in developed cities (GDP > 500 billion and population > 5 million) than in undeveloped cities (GDP < 10 billion and population < 0.5 million). Overall, the extreme LST thresholds were 36.16 ± 0.46 °C, 35.43 ± 1.62 °C, 35.34 ± 1.98 °C, 35.03 ± 1.96 °C and 35.14 ± 3.79 °C

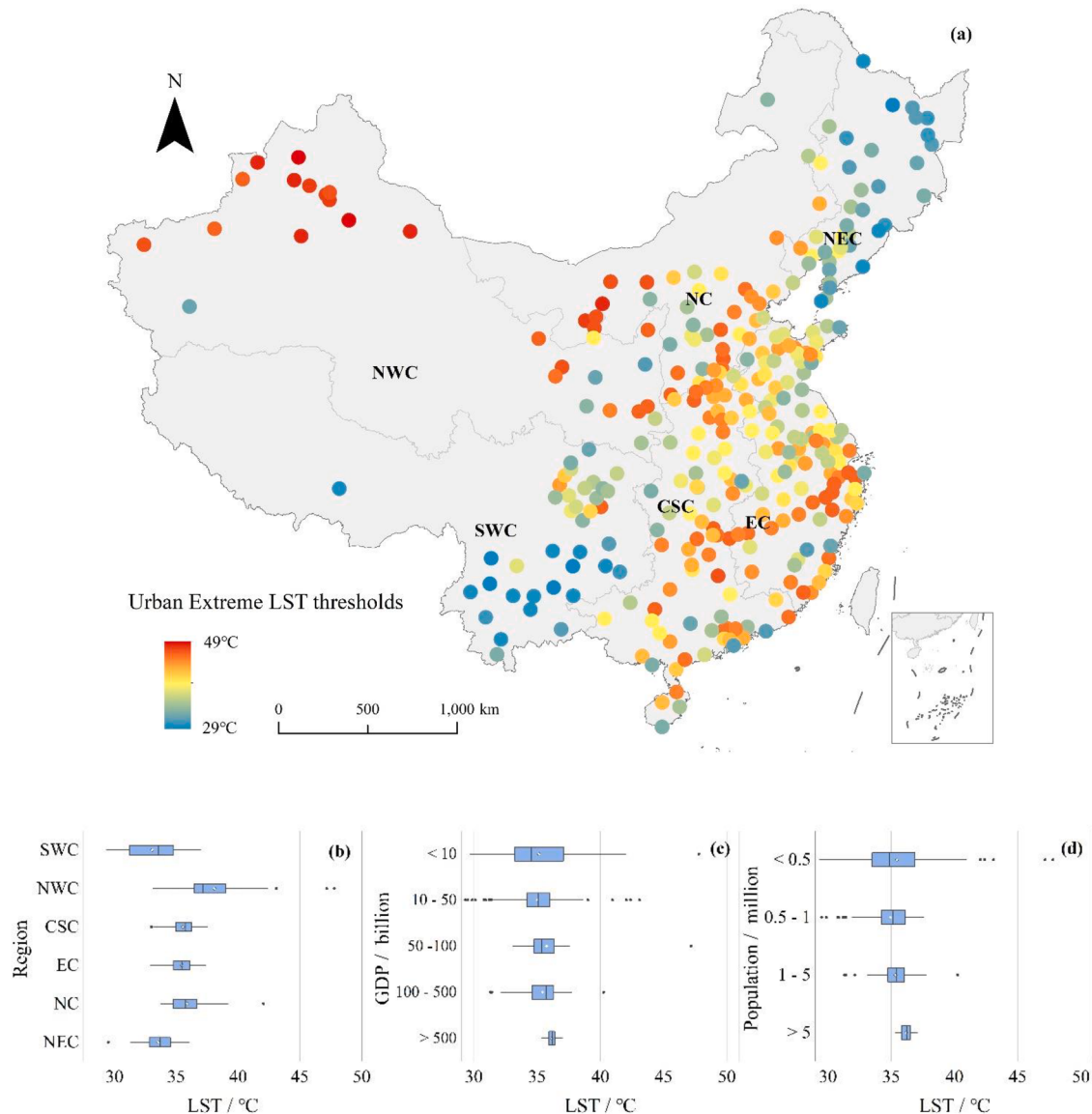


Fig. 3. The extreme LST thresholds for cities (a) Spatial distribution of extreme LST thresholds for cities in the study. (b) Box line diagram of extreme LST thresholds for different regions. (c) Box line diagram of extreme LST thresholds for different GDP. (d) Box line diagram of extreme LST thresholds for different populations. Note: map lines delineate study areas and do not necessarily depict accepted national boundaries

in cities with the GDP of > 500 billion, 100-500 billion, 50-100 billion, 10-50 billion and < 10 billion, respectively (Fig. 3c) and 36.19 ± 0.59 °C, 35.33 ± 1.24 °C, 34.95 ± 1.63 °C, and 35.44 ± 3.47 °C in cities with populations of > 5 million, 1 - 5 million, 0.5 - 1 million, and < 0.5 million, respectively (Fig. 3d).

3.2. Unevenness of urban population exposed to extreme heat (UPEEH)

The results showed that extreme heat-exposed areas increased exponentially each year. The extreme heat-exposed regions have increased by about 27.8 square kilometers since 2000, equivalent to an average increase of approximately 321.32 soccer fields per year (Fig. S1a). The number of cities with extreme heat exposure increases annually by approximately 2.59 cities per year. Between 2000 and 2020, the proportion of cities experiencing extreme heat increased from 77.8 % to 94.2 % (Fig. S1b).

During 2000-2020, approximately 80.94 % of the cities experienced extreme heat for over 15 consecutive years; approximately 72 cities had 21 straight years of LST exceeding the extreme LST threshold. Only two

cities had less than 10 years (Fig. 4a). The proportion of cities in EC with more than 15 consecutive years of extreme heat was relatively high, while the distribution of cities in other regions was even higher (Fig. 4b). Developed cities characterized by high GDP and large populations have a higher proportion of consecutive exposures to extreme heat, exceeding 15 years. In contrast, the balance of cities with fewer successive years of exposure to extreme heat was higher in cities with lower levels of urban development (Fig. 4c, 4d).

From 2000 to 2020, the population exposed to extreme heat increased by approximately 115 million in 320 cities, with the rate of increase accelerating after 2010 to an average of approximately 9.64 million people per year (Fig. 6a). Most cities (83.43 %) showed an upward trend in UPEEH. Interestingly, the annual percentage of urban population exposed to extreme heat decreased from 21.38 % to 14.28 % (Fig. 7a).

For the different regions, the larger number of UPEEH is concentrated in the Beijing-Tianjin-Hebei, Yangtze River Delta, and Pearl River Delta regions, where the economy is more developed. The population flow is higher (Fig. 5a). Among them, the number of UPEEH in EC (slope

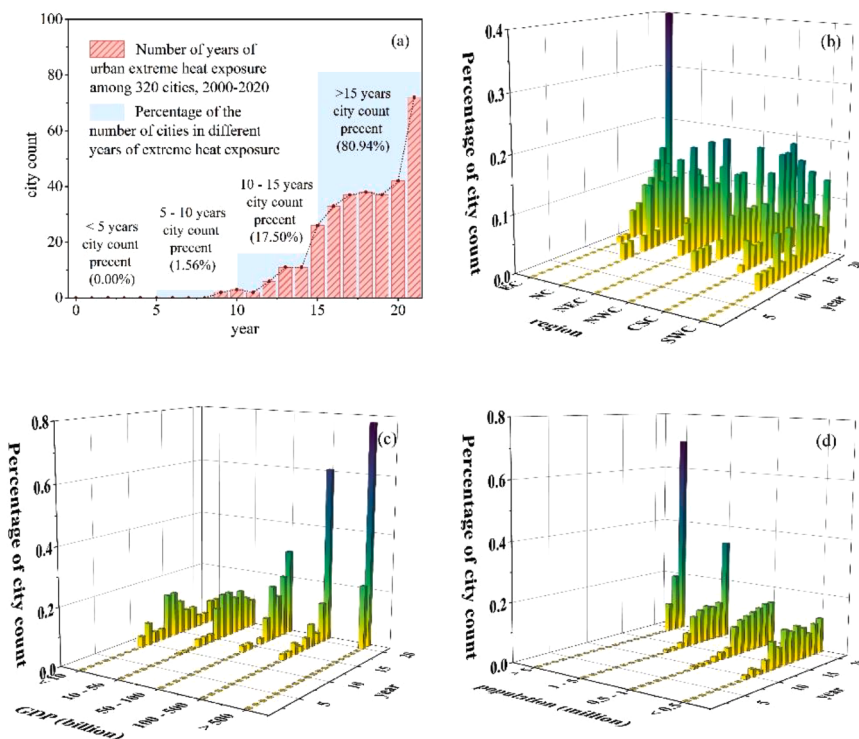


Fig. 4. Statistics on the years of continuous heat exposure in cities. (a) national; (b) region; (c) GDP; (d) population.

= 26944.074 people) and NC (slope = 28210.182 people) increased at a faster rate (Fig. 6b). Still, EC had the highest percentage (19.79 %) (Fig. 5b), yet the more considerable was the more rapid rate of decline (slope=-0.00564) (Fig. 7b). NC had the largest UPEEH (408,941.46 people). The next largest percentage (18.25 %) was after EC (Fig. 5b). The trend for the percentage of urban population exposed to extreme heat remained essentially unchanged (Fig. 7b). For NWC (slope = 1840.182 people) and NEC (slope = 5653.518 people), the UPEEH increased at a slower rate (Fig. 6b). Among them, NWC had the lowest UPEEH (109506.58 people) and percentage (10.86 %) (Fig. 5b), and the rate of decrease in percentage was slightly more pronounced (slope = -0.00214) (Fig. 7b). Still, PPHE in NEC showed an almost constant trend.

For the different GDP, the UPEEH was the largest in cities with a GDP greater than 500 billion and grew fastest (2,548,942.68 people, slope = 183,448.774) (Figs. 5c, 6c). The percentage of urban population exposed to extreme heat was the largest (22.99 %) (Fig. 5c). Still, the percentage decline was the fastest (slope = -0.00748) (Fig. 7c). Furthermore, cities with populations exceeding 5 million exhibited characteristics similar to those with GDPs exceeding 500 billion, with UPEEH and rates of change of 2,442,821.95 people (Fig. 5d) and 165,645.074 people (Fig. 6d), respectively, and the percentage of urban population exposed to extreme heat and rates of change of 22.63 % (Fig. 5d) and -0.00835 (Fig. 7d), respectively.

3.3. Spatiotemporal changes of urban extreme heat exposure risks

The UEHER index reflects the UEHER of cities from multiple perspectives (hazard, exposure, and vulnerability). The results of this study show that the national average UEHER index increased annually (Fig. 9a).

The spatial distribution of the UEHER index showed a gradual upward trend from southeast to northwest (Fig. 8a). In NWC, NC, and CSC, the UEHER exceeded the national average (Fig. 9b), and these three regions had a high proportion of medium, medium-high, and high risks increase, with the highest proportion of high-risk cities (3 %) in NC (Fig. 10a). In contrast, coastal and high-elevation areas such as EC, NEC,

and SWC had lower average UEHER indices (Fig. 9b). The difference was that EC and NEC had a relatively high proportion of low and medium-low risk (approximately 80 % or more). In contrast, SWC had a high proportion of medium- and medium-high risk and the largest proportion of low risk (Fig. 10a). However, the distribution of different GDP exceeded our expectations. As the GDP of cities increased, the UEHER index of cities showed an inverted v distribution (Fig. 9c), with the highest average UEHER index of cities when the GDP was medium; however, a smaller percentage of cities had high and medium-high risk (Fig. 10b). For cities with different populations, the UEHER index of cities showed a positive v distribution as the urban population increased (Fig. 9d). When the population was larger than 5 million and smaller than 0.5 million, the average UEHER index of cities was relatively high, and the ratio of high to medium-high risk was relatively high. The percentage of the low-risk index was highest in cities with an urban population of less than 0.5 million (Fig. 10c).

Understanding the changing trends in the UEHER is important for guiding future climate change. The UEHER deteriorated more rapidly in southern China. Almost all cities in China (approximately 97.19 %) showed an increasing trend in the UEHER index, mainly in SWC, EC, and CSC (Fig. 8b). Overall, the number of low-risk cities significantly decreased. In contrast, the number of medium-low-risk cities slowly decreased. Additionally, cities with medium risk rapidly increased and became more widespread in recent years (after 2010), with medium-to high-risk and high-risk cities becoming more prevalent (Fig. 11). The regions with faster trends in the UEHER index were concentrated in EC, SWC, and CSC (Fig. 9b). Cities with low risk in SWC declined the fastest, whereas cities with medium and high risk in CSC and EC increased the most immediate. The cities in other regions did not change significantly (Fig. 11b, j, and r). For cities with different GDP, the UEHER index changed the fastest for cities with a GDP of 50–100 billion, slower in developed cities, and slowest in underdeveloped cities (Fig. 9c). It is worth noting that changes in the number of low, low-medium, medium, and medium-high risk cities were most pronounced in cities with a GDP of 10–50 billion (Fig. 11c, g, k, o), and most cities with a GDP of 10–50 billion transitioned from low to medium risk. However, an increase in

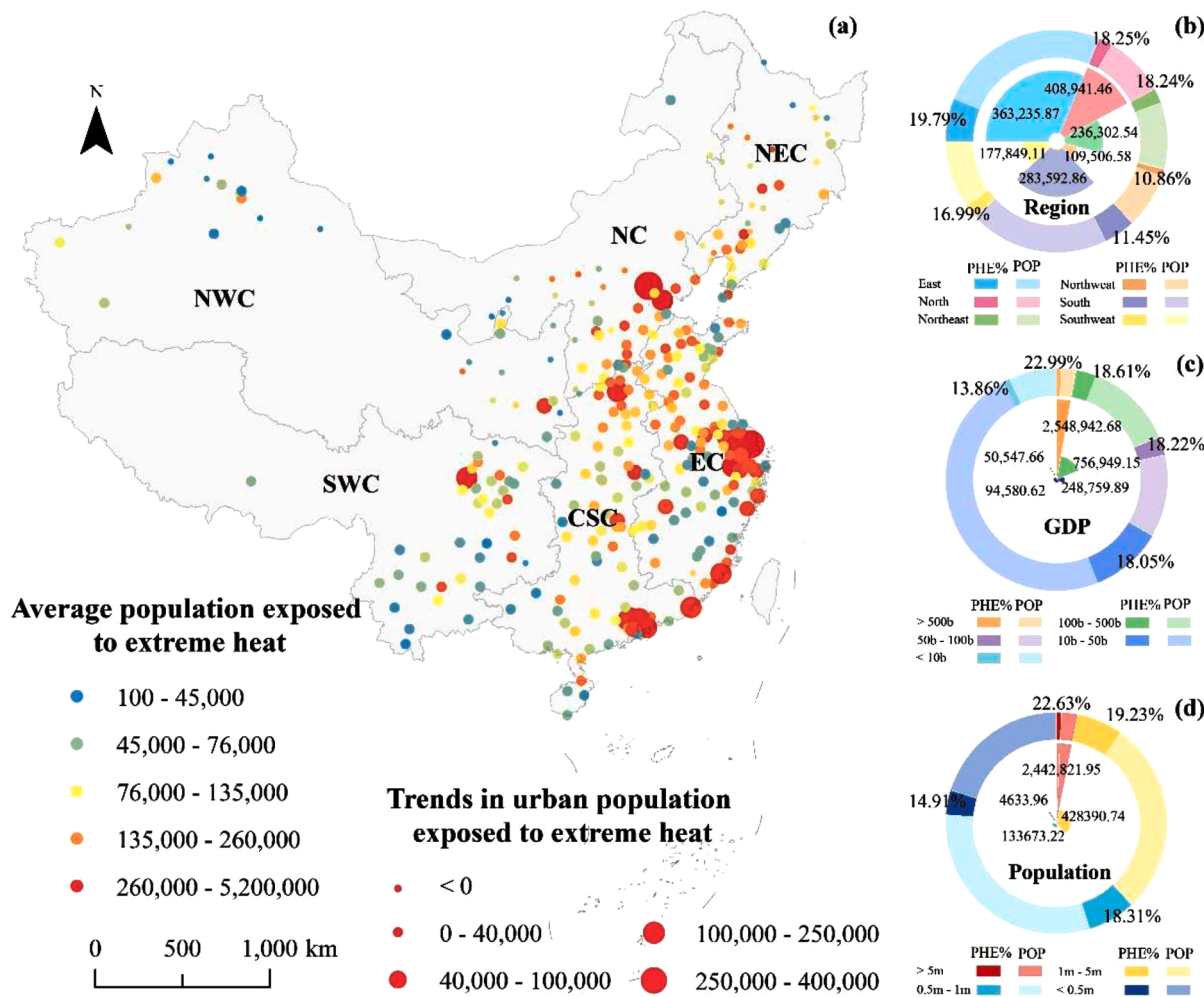


Fig. 5. Changes in urban UPEEH. (a) Spatial distribution of urban UPEEH. (b) Statistics of UPEEH in different regions. (c) Statistics of UPEEH for different GDPs. (d) Statistics of UPEEH for different populations. Note: The rose diagram represents the statistics of the number of UPEEH in different city types, and the percentage of different colors in the external ring diagram represents the percentage of the number of different types of cities, where the dark shade indicates the percentage of UPEEH and the light color indicates the percentage of non-UPEEH. Note: map lines delineate study areas and do not necessarily depict accepted national boundaries

high-risk cities was only observed in cities with a GDP of 100–500 billion (Fig. 11s). For different urban populations, the trend in the UEHER slowed as the urban population decreased (Fig. 9d). Most cities with populations of 1–5 million, 0.5–1 million, <0.5 million were similarly in the process of transitioning from low to medium or even medium-high risk, and some cities with populations of 1–5 million had already transitioned to high risk (Fig. 11d, h, l, p, t). The change in the risk level for developed cities (GDP > 500 billion, population > 5 million) was not significant.

4. Discussions

Our study confirms significant variations in extreme LST thresholds among cities. Lower thresholds were observed in the NEC and SWC, whereas higher thresholds were found in the belt, extending from the EC to the NWC. This variation is primarily attributed to natural geographical factors. The NWC is positioned at higher latitudes and is affected by Siberia's cold climate, which leads to cold winters and relatively short, cooler summers. Conversely, the SWC, situated at high altitudes and near mountainous areas, experiences blockage of northward tropical and subtropical air currents (Han et al., 2022). It is important to note that lower LST thresholds in the NEC and SWC do not imply the absence of hot weather but rather comparatively milder summer temperatures (Zhou et al., 2022). In contrast, the NWC lies inland, distant from

oceanic regulations, and lacks the influence of maritime air currents. With mostly plateau and basin topographies, direct sunlight, strong ground radiation, and heat conduction result in higher summer temperatures (Feng et al., 2023; Freychet et al., 2022). The EC, CSC, and NC, located in the mid-latitude zone, experience increased direct sunlight and longer sunshine hours during summer (Sadeghi et al., 2021). They are influenced by the Siberian high pressure and Pacific subtropical high pressure, leading to sinking air currents, heightened surface pressure, and temperatures. While geographic location and climatic conditions significantly affect urban thermal changes, social factors also interfere (Kong et al., 2014). Developed economies and high urbanization cause heat release from human activities, such as buildings, population, and traffic, amplifying the UHI effect and inevitable urban temperature rise.

Residents have different tolerances and sensitivities to heat extremes in different regions, and some studies have already shown that residents of regions with hot summers and cold winters are the most tolerant to changes in the thermal environment (Sun et al., 2023; Zhi et al., 2021). However, only the combination of extreme LST thresholds and population can accurately represent residents' living standards and comfort levels (McElroy et al., 2020; Ullah et al., 2022), which is crucial for guiding urban development. The number of people affected by extreme heat has increased, especially after 2010 (Fig. 6). However, the number of people threatened by extreme heat as a proportion of the total population shows a decreasing trend (Fig. 7). There are three possible

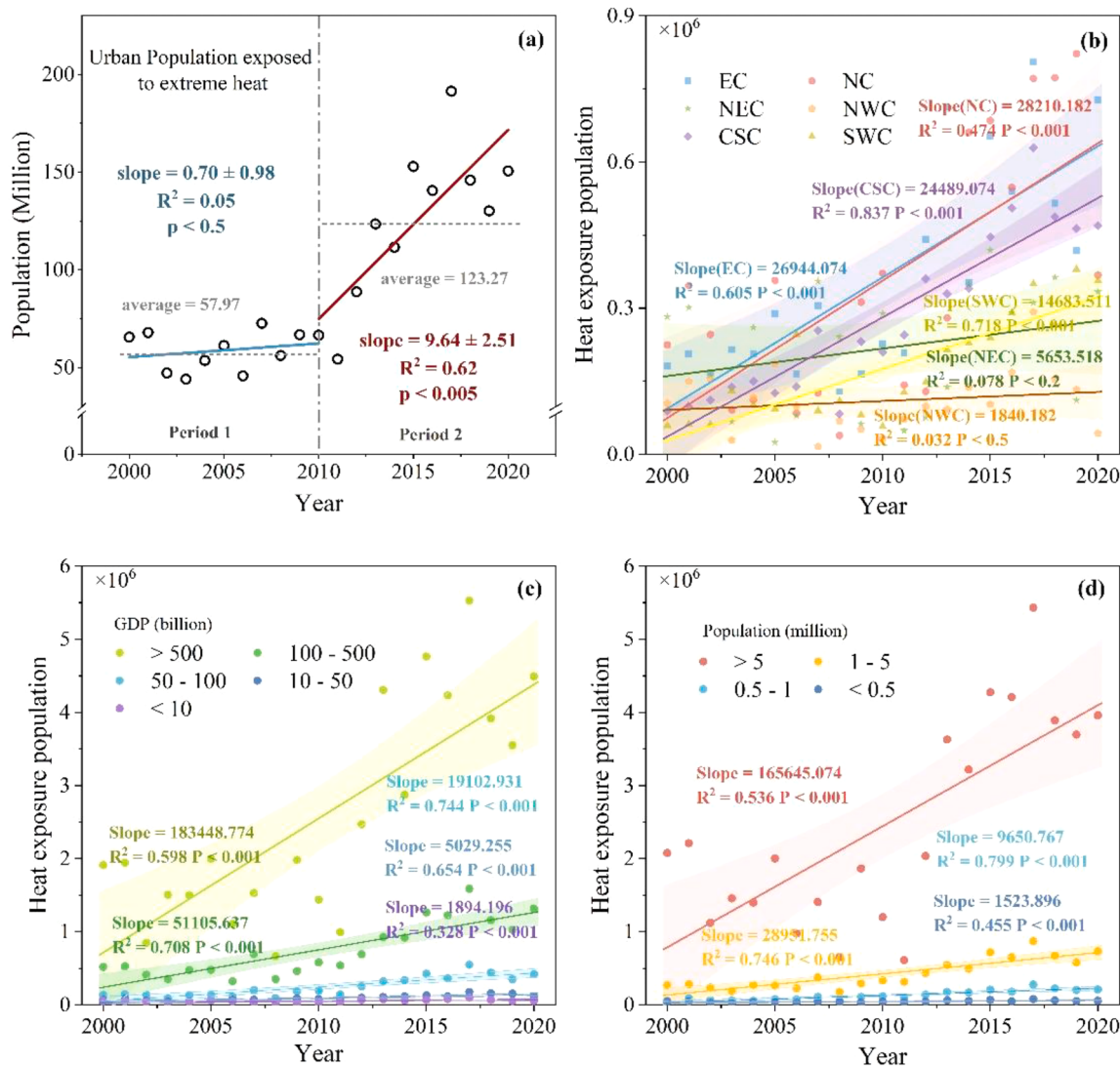


Fig. 6. Annual changes in the total number of UPEEH in the cities studied. (a) national; (b) region; (c) GDP; (d) population.

explanations for this. First, urbanization attracts rural populations. An increase in the number of urban residents leads to a decrease in the number of people threatened by extreme heat as a proportion of the total population, in other words, the number of urban residents increases at a much faster rate than the increase in the population threatened by extreme heat exposure (Freychet et al., 2022; Klein & Anderegg, 2021). Second, more and more residents tend to live in suburban or newly developed urban areas, transforming the areas in which they work and live to improve their living conditions, while city centers are transformed into commercial areas. This is a general trend, however, with some variations between cities (Freychet et al., 2022; Klein & Anderegg, 2021). Thirdly, the green urban policy such as Forest city establishment is proposed in China (Pei et al., 2019). The fact that urban green spaces are increasing is also confirmed by many studies (Sun et al., 2020), which shows that the proposed policies are being implemented and are effective. Most studies have shown that urban green spaces can reduce the risk of population exposure to extreme heat (Wang et al., 2023a). Our study shows a downward trend in the proportion of the population exposed to extreme temperatures, which also confirm the success of the proposed urban greening policy in dealing with urban heat waves. In the northeastern, northwestern, and southwestern regions of China, slower UPEEH growth occurred because of less development, and the migration of young people to developed cities reduced UPEEH growth in these

areas. Interestingly, the PUPEEH did not decline significantly in northeastern and NC. NEC is experiencing more severe population loss, whereas North China is experiencing more population influx and has experienced frequent extreme heat events in recent years.

Urban heat waves pose an escalating threat, increasing heat-affected city populations (Kephart et al., 2022). It can cause heat-related deaths and indirectly other diseases, such as cardiovascular and respiratory diseases (Ruiz-Paez et al., 2023; Wang et al., 2019). Considering the limitations of urban mortality data collection, we applied the publicly available 2013 mortality data from various causes in another study to verify the accuracy of the results of this study (Fang et al., 2016) and selected 68 cities as the study population to explore the relationship between the UEHER index and disease mortality. The 68 cities had a risk ranging from approximately 0–0.4 were at low and medium-low risk. The results showed that the average mortality rate for all diseases in cities in the medium-low risk zone was approximately five times higher than in the low-risk zone, and for respiratory diseases, lung cancer, and cardiovascular diseases, the medium-low risks were about 3.7, 4.6, and 3 times higher than the low risks, respectively. (Fig. S2). The UEHER showed a significant positive correlation with respiratory diseases ($P < 0.05$) (Fig. S2c) and lung cancer ($P < 0.005$) (Fig. S2d). This is because high temperature and humidity may lead to discomfort such as shortness of breath and chest tightness, especially for the elderly, children, and

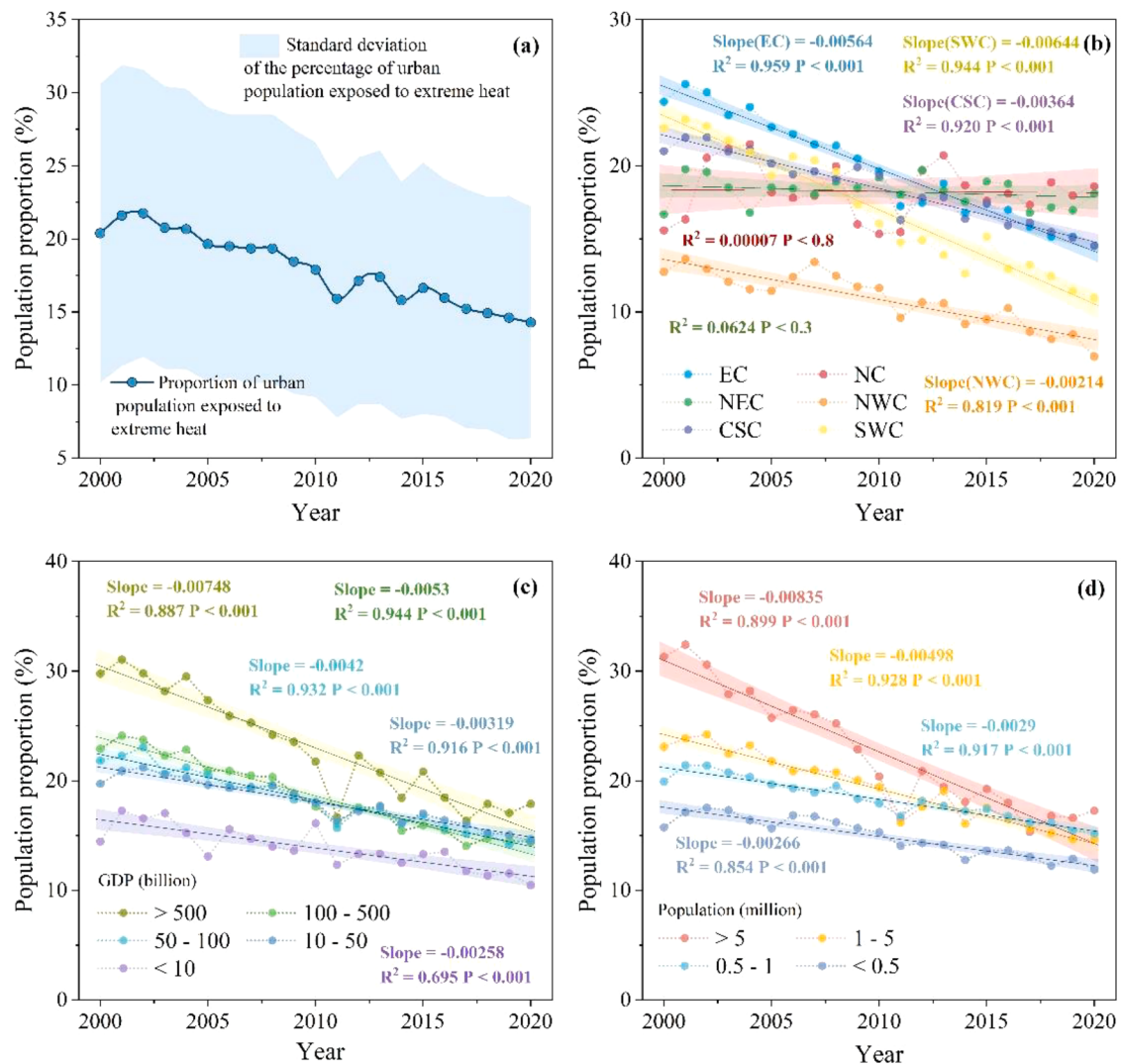


Fig. 7. Percentage of population exposed to extreme heat per year. (a) national; (b) region; (c) GDP; (d) population.

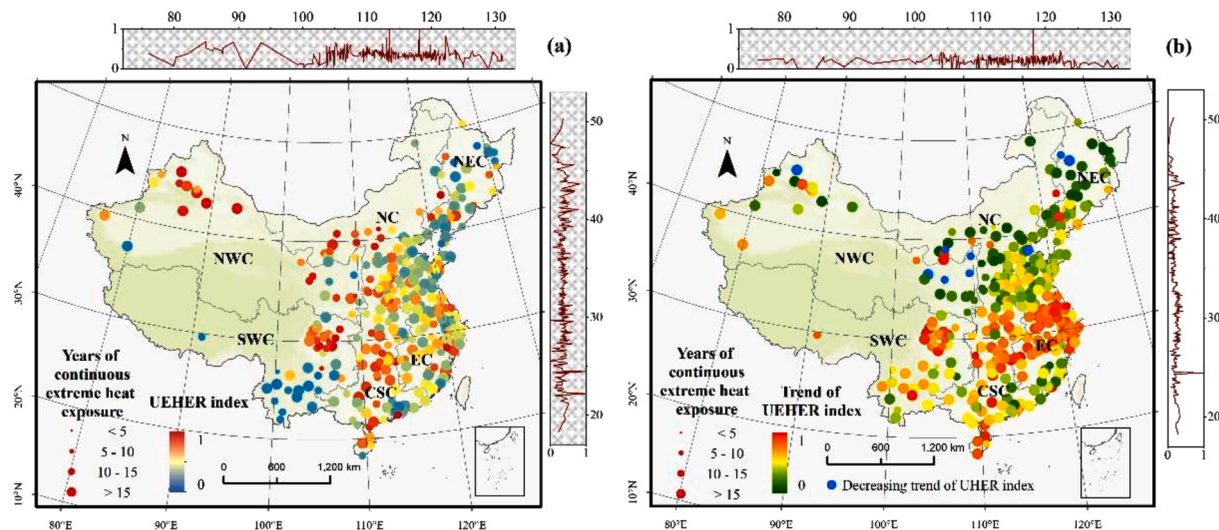


Fig. 8. Distribution of UEHER index. (a) Spatial variation of UEHER index. (b) Changes in UEHER index over time. Note: map lines delineate study areas and do not necessarily depict accepted national boundaries

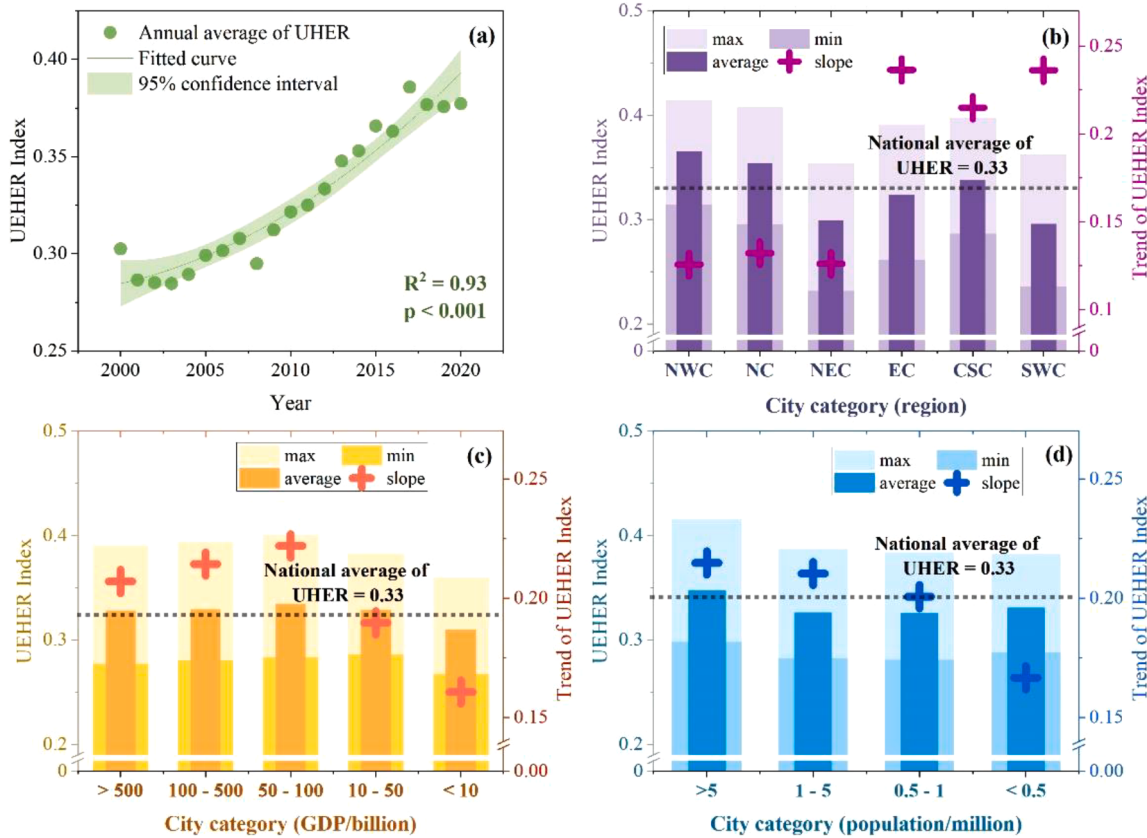


Fig. 9. Changes in the UEHER index. (a) Change in annual average UEHER index (b) UEHER index and trends in different regions (c) UEHER index and trends in different GDP (d) UEHER index and trends in different population

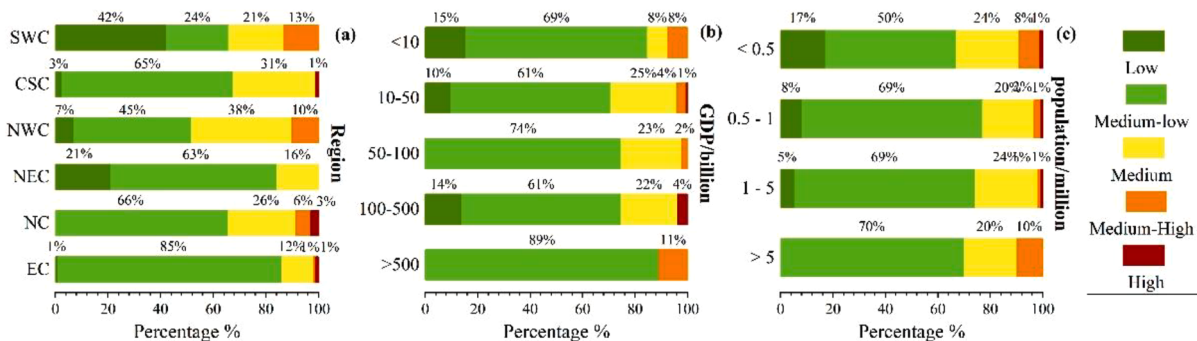


Fig. 10. Percentage of the urban extreme heat exposure risk level in different city categories. (a) regions. (b) GDP. (c) population.

patients with respiratory diseases, in addition to increasing the risk of lung cancer due to the accumulation of urban heat and pollutant emissions, which may exacerbate air pollution (Han et al., 2022; Ikaheimo et al., 2020). However, a negative but non-significant trend ($P < 0.2$) (Fig. S2b) was observed for cardiovascular diseases, which could be attributed to heightened mortality from lifestyle habits and vasoconstriction in colder climates. Dehydration and increased blood viscosity at high temperatures may also play a role (Guo et al., 2023; Ikaheimo et al., 2020; Liu et al., 2022), thereby straining the heart and blood vessels, potentially leading to heart disease and stroke (Cleland et al., 2023; Psistaki et al., 2023).

The UEHER study results reveal a dual crisis of high UEHER and rapid deterioration in medium-economically developed, densely populated cities, such as CSC and EC. Many studies have shown that the UEHER is higher in less-developed cities (Chakraborty et al., 2019;

Freychet et al., 2022; Hsu et al., 2021), which aligns with our findings that developed cities often possess better coping strategies. However, most of these studies have concentrated on developed nations, whereas China is still a developing country, making its cities comparatively less developed. Cities in China have been experiencing rapid urbanization from 2000-2020, with increasing population densities and expanding city scales (Wang et al., 2023b). This growth has prompted medium-sized developed cities to encounter heightened energy demands, particularly in the industrial and transportation sectors. Increased energy consumption and emissions have amplified air pollution and GHG emissions. In addition, infrastructure development may be delayed, such as the lack of adequate green space and tree cover, lack of urban wetlands and water bodies, and lack of sound urban planning and building design, all of which contribute to the inability of cities to regulate temperature and heat effectively (Zhou et al., 2021). Moreover,

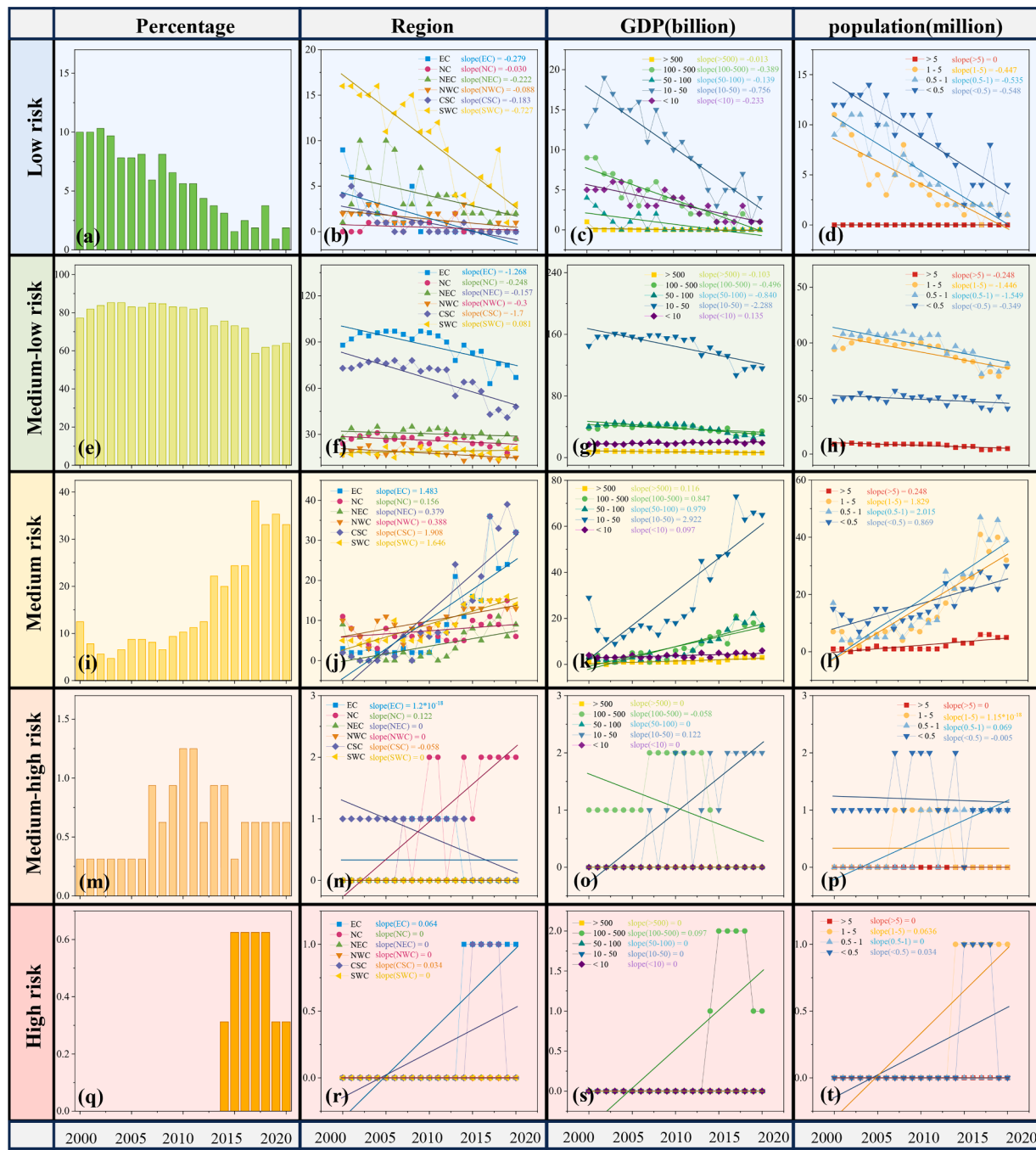


Fig. 11. Trend of urban extreme heat exposure risk level in different city categories, where the bars represent the percentage of cities with varying levels of risk in different years, dotted line graphs represent the number of cities in different city types

research corroborates our findings by noting a significant decline in the population exposed to greenfield cooling in medium- and less-developed Chinese cities (Dong et al., 2022); in other words, the UEHER in such cities is high and changing rapidly, corroborating the findings of this study. In contrast, there is still a gap between less-developed cities in China and less-developed cities abroad; therefore, the UEHER in less-developed cities in China is lower than that in other studies.

The UEHER requires attention to the double inequality faced by residents of less-developed cities, a higher UEHER, and a lower standard of living (Chakraborty et al., 2019; Sun et al., 2020). This scenario is evident in cities with lower population densities and GDP in Northwest China. Economic, technological, and infrastructure limitations often plague less-developed regions, impeding their capacity to adapt and

mitigate the UEHER. However, it is fortunate for the inhabitants living in these regions that the annual rate of change in the UEHER is slower, and this region usually has a relatively low population density, slower urbanization and population growth, and a slower response to climate warming. Therefore, there is an urgent need to develop a well-designed adjustment strategy for the region to reduce the double inequality of its inhabitants and ensure the sustainable development of less-developed areas and the well-being of its people.

Although the UEHER cannot be eliminated in terms of adaptation planning, corresponding measures can reduce the UEHE, vulnerability, and sensitivity while improving the coping capacity and resilience of cities. The normalized slope of the change between the UEHER index and the influencing factors shows that the UEHER index increases more

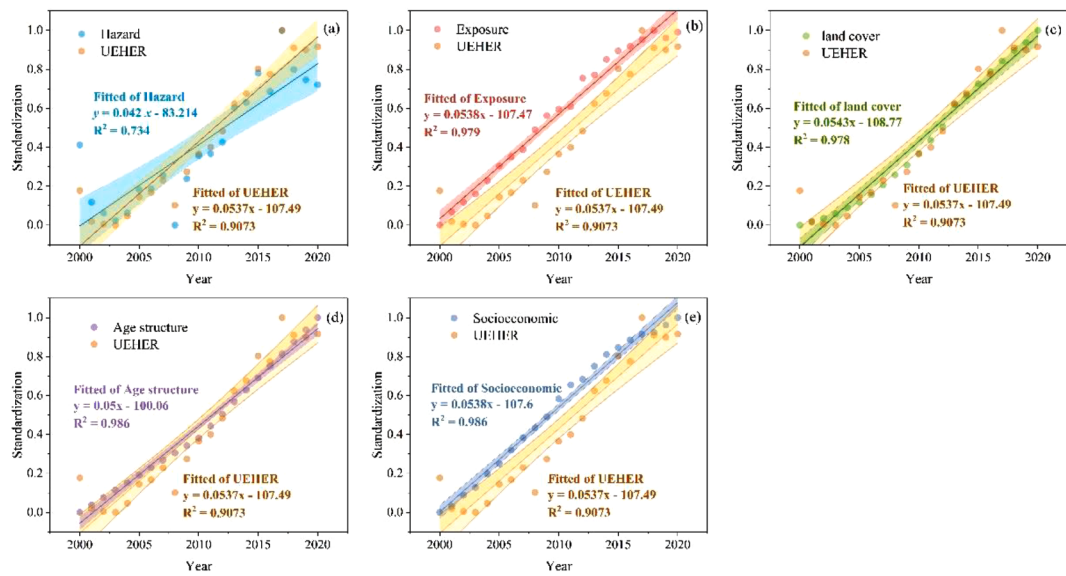


Fig. 12. Relationship between trends in urban extreme heat exposure risk index and influencing factors. (a) hazard; (b) exposure; (c) age structure; (d) land cover; (e) socioeconomic.

slowly than the changes in population, economic growth, and the proportion of impervious areas (Fig. 12b, c, e), which implies that these three factors primarily contribute to the UEHER increase. In addition, it is faster than the changes in population aging and urban heat hazards (Fig. 12a, d).

Indeed, while nighttime temperatures are not as high as daytime temperatures, their adverse effects on human health are often overlooked. Nighttime heat affects sleep, and studies have found that people are waking up more often from heat (Minor et al., 2022), especially older people and women, and that nighttime heat leads to more sleep loss, increases fatigue, makes people more susceptible to heat stress and exacerbates disease morbidity and mortality (Ullah et al., 2022). Studies have shown a significant positive correlation between short-term exposure to hot nights and mortality in the population, with nighttime heat still increasing the risk of death by 40 % to 50 % (He et al., 2022). Our study found that the risk of daytime heat exposure is largely positively correlated spatially with the risk of nighttime heat exposure, which is only about 10 % smaller than the daytime risk, and that the impact of nighttime heat should not be underestimated, especially in areas where the daytime risk is higher (Fig. 13).

Utilizing green spaces as infrastructure is a vital approach to address the UEHER, as urban green areas offer ecological services, such as enhancing the urban environment and regulating the local climate (Massaro et al., 2023; Wang et al., 2022b). A significant relationship emerged through a study analyzing urban greenspace coverage and the UEHER from 2000 to 2020: higher urban green space coverage correlated with lower UEHER index values. This relationship exhibits a negative logarithmic trend. Specifically, there is a rapid decrease in the UEHER between green space coverages of 0 and 0.2. In contrast, the reduction in the UEHER becomes gradual after reaching a green space coverage of approximately 0.5 (Fig. S3).

Moreover, although reducing the urban population in developed areas presents challenges, alleviating extreme heat exposure requires proactive policies that foster regional growth and development. This would naturally encourage young individuals to choose other cities for opportunities, distribute the population more evenly, and reduce their concentration in developed urban centers. Another issue requiring attention is the aging population. Some studies show that older people and children are less resilient and that the heat death rate of the non-working age population is about 3.58 times higher than that of the

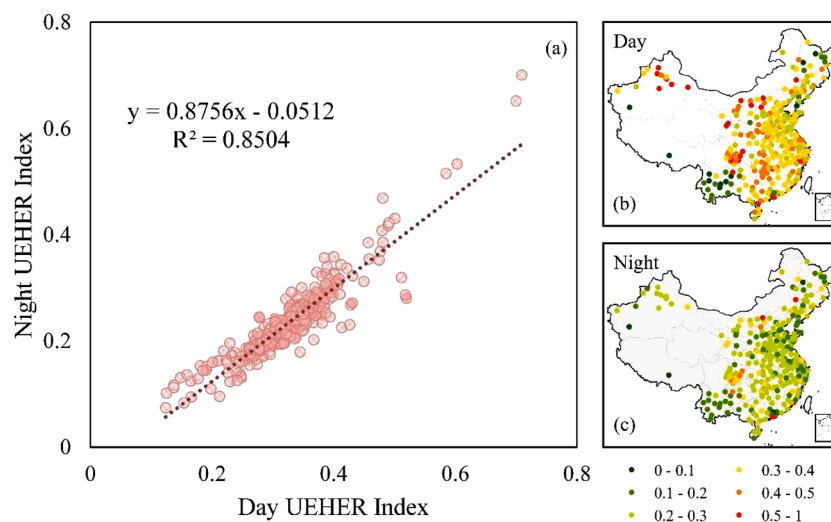


Fig. 13. Variation in UEHER index during the day and at night.

working age population (Chen et al., 2023; Wang et al., 2019; Zhu & Yuan, 2023). Special attention should be paid to cities with high levels of aging population. Examples include improving housing conditions for socially vulnerable groups, improving the community infrastructure, and providing appropriate emergency assistance and health coverage to ensure protection and support during hot weather.

This will involve a very important issue, which is population growth, migration, and transition, whereas the pursuit of quality of life fundamentally requires education, work, housing, health, leisure, and mobility, which are considered to be the core elements of sustainability-based development, the neglect of which may undermine improvements in the quality of life of the population, thus putting the necessary governance and governability on hold. Thus, the need to mitigate urban heat exposure is as complex as the productive reality. In addition, the availability of knowledge, tools, and technologies, among others, can provide a solid foundation for decision-making processes at all levels and must be vigorously developed to facilitate the establishment of integrated development systems as an important adjunct to the achievement of sustainable development goals. Specifically, public health alerts and emergency responses in areas of severe ageing contribute to safer, more sustainable, and resilient urban environments for vulnerable groups.

While land-use change is central to urbanization, comprehensive urban planning policies must prioritize reducing high-density buildings and concrete usage (Wu et al., 2022). Especially in cities with large numbers of population exposed to extreme thermal environments, both indoor and outdoor cooling need to be considered. For indoors, enhancing the availability of public air conditioning or other cooling equipment improves the comfort of indoor residents. However, since some residents may unavoidably work outdoors, the heat generated by air conditioning can increase outdoor discomfort. For the outdoors, enhance ventilation, improve shading facilities, the construction of blue-green spaces, or try to develop new technologies to convert the heat generated by air conditioning.

It should be acknowledged that there are limitations to this study. Although the correlation between LST and air temperature is strong, there is still some variability in the study of extreme heat exposure, while air temperature more directly reflects human comfort. Therefore, in future studies, we should set up as many monitoring stations as possible and pay more attention to the acquisition of data from monitoring stations. In addition, regarding the assessment of extreme heat thresholds, although we have calculated the extreme heat thresholds for each city based on scientific assessment methods, there is a certain degree of uncertainty in the extreme heat thresholds we have derived due to the fact that each individual has a different degree of sensitivity to extreme heat. Moderate-resolution MODIS temperature data (1000 m) may lead to underestimating extreme LST thresholds. Future research should focus on high-precision, long-term LST data. Due to the limitations of the data, the extent and use of air conditioning needs to be taken into account when exploring heat stress in the population in future studies, which will improve the accuracy of the data reflecting heat stress in the population.

5. Conclusion

This study revealed significant differences in the increasing risk of extreme heat exposure across different urban categories, raising substantial challenges of imbalance and vulnerability for urban residents to cope with the urban thermal environment.

This study explored the extreme LST thresholds for each city, which could help develop effective public health alerts and emergency response measures. The temperature range of extreme LST thresholds in the studied cities is 29.32 °C–47.79 °C, with an average of 35.24 °C. Relatively high extreme LST thresholds were concentrated in the northwest, at higher economic levels, and in high-density populations. From 2000 to 2020, the number of urban residents exposed to extreme

heat increased by approximately 115 million over 20 years, with larger increases occurring in eastern and northern Chinese cities. However, the percentage of urban population exposed to extreme heat decreased from 21.38 % to 14.28 %, with significant changes concentrated in developed cities such as those in EC.

Compared to 2000, the UEHER index will increase by approximately 52.5 % by 2020. The UEHER gradually increased from the coastal to inland cities. The UEHER deteriorated faster in southern China. In China, central-south cities, medium-GDP cities, and cities with high population densities face the dual risks of high extreme heat exposure and rapid deterioration. In contrast, northwest China and less-developed regions face the double inequality of high UEHER and low GDP.

Our approach is broad and can provide recommendations and reflections for other countries and regions. Considering the inadequate infrastructure and lack of capacity to cope with adverse environments in underdeveloped cities, greater attention should be paid to the issue of unequal well-being among residents in these areas. For medium and developed cities, where population influx, rapid development, and severe aging occur, it is crucial to enhance risk-mitigation strategies, especially for the health of vulnerable groups. This study contributes to developing safer, sustainable, and resilient urban environments.

CRediT authorship contribution statement

Chengcong Wang: Writing – original draft, Visualization, Methodology, Formal analysis, Conceptualization. **Zhibin Ren:** Writing – review & editing, Supervision, Methodology, Funding acquisition, Conceptualization. **Yujie Guo:** Investigation, Data curation. **Peng Zhang:** Software, Formal analysis. **Shengyang Hong:** Methodology, Data curation. **Zijun Ma:** Validation, Investigation. **Wenhai Hong:** Investigation. **Xinyu Wang:** Formal analysis.

Declaration of competing interest

The authors declare that they have no known competing financial interests or personal relationships that could have appeared to influence the work reported in this paper.

Data availability

I've shared the data and link at the attach file.

Acknowledgements

This work was supported by the National Natural Science Foundation of China [grant number 42171109, 32130068], the Youth Innovation Promotion Association of Chinese Academy of Sciences [grant number 2020237], the National Key R&D Program of China [grant number 2023YFF1304604].

Supplementary materials

Supplementary material associated with this article can be found, in the online version, at [doi:10.1016/j.scs.2024.105260](https://doi.org/10.1016/j.scs.2024.105260).

References

- Cao, J., Zhou, W., Yu, W., Hu, X., Yu, M., Wang, J., & Wang, J. (2022). Urban expansion weakens the contribution of local land cover to urban warming. *Urban Climate*, 45. <https://doi.org/10.1016/j.uclim.2022.101285>
- Cao, Z., Wu, Z., Li, S., Guo, G., Song, S., Deng, Y., Ma, W., Sun, H., & Guan, W. (2020). Explicit spatializing heat-exposure risk and local associated factors by coupling social media data and automatic meteorological station data. *Environmental Research*, 188, Article 109813. <https://doi.org/10.1016/j.envres.2020.109813>
- Chakraborty, T., Hsu, A., Manya, D., & Sheriff, G. (2019). Disproportionately higher exposure to urban heat in lower-income neighborhoods: A multi-city perspective. *Environmental Research Letters*, 14. <https://doi.org/10.1088/1748-9326/ab3b99>

- Chen, B., Xie, M., Feng, Q., Wu, R., & Jiang, L. (2022a). Diurnal heat exposure risk mapping and related governance zoning: A case study of Beijing, China. *Sustainable Cities and Society*, 81. <https://doi.org/10.1016/j.scs.2022.103831>
- Chen, H., Zhao, L., Cheng, L., Zhang, Y., Wang, H., Gu, K., Bao, J., Yang, J., Liu, Z., Huang, J., Chen, Y., Gao, X., Xu, Y., Wang, C., Cai, W., Gong, P., Luo, Y., Liang, W., & Huang, C. (2022b). Projections of heatwave-attributable mortality under climate change and future population scenarios in China. *The Lancet regional Health Western Pacific*, 28, Article 100582. <https://doi.org/10.1016/j.lanwpc.2022.100582>
- Chen, M., Chen, L., Zhou, Y., Hu, M., Jiang, Y., Huang, D., Gong, Y., & Xian, Y. (2023). Rising vulnerability of compound risk inequality to ageing and extreme heatwave exposure in global cities. *NPJ Urban Sustainability*. <https://doi.org/10.1038/s42949-023-00118-9>
- Chen, S., Yu, Z., Liu, M., Da, L., & Faiz Ul Hassan, M. (2021). Trends of the contributions of biophysical (climate) and socioeconomic elements to regional heat islands. *Scientific Reports*, 11, 12696. <https://doi.org/10.1038/s41598-021-92271-3>
- Cheng, Q., Jin, H., & Ren, Y. (2023a). Compound daytime and nighttime heatwaves for air and surface temperature based on relative and absolute threshold dynamic classified in Southwest China, 1980–2019. *Sustainable Cities and Society*, 91. <https://doi.org/10.1016/j.scs.2023.104433>
- Cheng, Y., Yu, Z., Xu, C., Manoli, G., Ren, X., Zhang, J., Liu, Y., Yin, R., Zhao, B., & Vejre, H. (2023b). Climatic and economic background determine the disparities in urbanites' expressed happiness during the summer Heat. *Environmental Science & Technology*, 57, 10951–10961. <https://doi.org/10.1021/acs.est.3c01765>
- Cheval, S., Dumitrescu, A., Amihăesci, V., Iraşoc, A., Paraschiv, M.-G., & Ghent, D. (2023). A country scale assessment of the heat hazard-risk in urban areas. *Building and Environment*, 229. <https://doi.org/10.1016/j.buildenv.2022.109892>
- Cleland, S. E., Steinhardt, W., Neas, L. M., Jason West, J., & Rappold, A. G. (2023). Urban heat island impacts on heat-related cardiovascular morbidity: A time series analysis of older adults in US metropolitan areas. *Environment International*. <https://doi.org/10.1016/j.envint.2023.108005>
- Dong, Y., Ren, Z., Fu, Y., Hu, N., Guo, Y., Jia, G., & He, X. (2022). Decrease in the residents' accessibility of summer cooling services due to green space loss in Chinese cities. *Environment International*, 158. <https://doi.org/10.1016/j.envint.2021.107002>
- Dou, Y., & Kuang, W. (2020). A comparative analysis of urban impervious surface and green space and their dynamics among 318 different size cities in China in the past 25 years. *Science of the Total Environment*, 706, Article 135828. <https://doi.org/10.1016/j.scitotenv.2019.135828>
- Estoque, R. C., Ooba, M., Seposo, X. T., Togawa, T., Hijioka, Y., Takahashi, K., & Nakamura, S. (2020). Heat health risk assessment in Philippine cities using remotely sensed data and social-ecological indicators. *Nature Communications*, 11, 1581. <https://doi.org/10.1038/s41467-020-15218-8>
- Fang, D., Wang, Q., Li, H., Yu, Y., Lu, Y., & Qian, X. (2016). Mortality effects assessment of ambient PM_{2.5} pollution in the 74 leading cities of China. *The Science of the Total Environment*, 569–570, 1545–1552. <https://doi.org/10.1016/j.scitotenv.2016.06.248>
- Feng, R., Wang, F., Liu, S., Qi, W., Zhao, Y., & Wang, Y. (2023). How urban ecological land affects resident heat exposure: Evidence from the mega-urban agglomeration in China. *Landscape and Urban Planning*, 231. <https://doi.org/10.1016/j.landurbplan.2022.104643>
- Flöttum, K., Gasper, D., & St. Clair, A. L. (2016). Synthesizing a policy-relevant perspective from the three IPCC "Worlds"—A comparison of topics and frames in the SPMs of the Fifth Assessment Report. *Global Environmental Change*, 38, 118–129. <https://doi.org/10.1016/j.gloenvcha.2016.03.007>
- Freychet, N., Hegerl, G. C., Lord, N. S., Lo, Y. T. E., Mitchell, D., & Collins, M. (2022). Robust increase in population exposure to heat stress with increasing global warming. *Environmental Research Letters*, 17. <https://doi.org/10.1088/1748-9326/ac71b9>
- Guo, M., Yu, W., Zhang, Y., Li, B., Zhou, H., & Du, C. (2023). Associations of household dampness and cold exposure with cardiovascular disease and symptoms among elderly people in Chongqing and Beijing. *Building and Environment*, 233. <https://doi.org/10.1016/j.buildenv.2023.110079>
- Han, C., Xu, R., Ye, T., Xie, Y., Zhao, Y., Liu, H., Yu, W., Zhang, Y., Li, S., Zhang, Z., Ding, Y., Han, K., Fang, C., Ji, B., Zhai, W., & Guo, Y. (2022). Mortality burden due to long-term exposure to ambient PM(2.5) above the new WHO air quality guideline based on 296 cities in China. *Environment International*, 166, Article 107331. <https://doi.org/10.1016/j.envint.2022.107331>
- He, C., Kim, H., Hashizume, M., Lee, W., Honda, Y., Kim, S. E., Kinney, P. L., Schneider, A., Zhang, Y., Zhu, Y., Zhou, L., Chen, R., & Kan, H. (2022). The effects of night-time warming on mortality burden under future climate change scenarios: A modelling study. *The Lancet Planetary health*, 6, e648–e657. [https://doi.org/10.1016/S2542-5196\(22\)00139-5](https://doi.org/10.1016/S2542-5196(22)00139-5)
- Hsu, A., Sheriff, G., Chakraborty, T., & Manya, D. (2021). Disproportionate exposure to urban heat island intensity across major US cities. *Nature Communications*, 12, 2721. <https://doi.org/10.1038/s41467-021-22799-5>.
- Hu, L., Wilhelmi, O. V., & Uejio, C. (2019). Assessment of heat exposure in cities: Combining the dynamics of temperature and population. *Science of the Total Environment*, 655, 1–12. <https://doi.org/10.1016/j.scitotenv.2018.11.028>
- Huang, H., Ma, J., & Yang, Y. (2023). Spatial heterogeneity of driving factors for urban heat health risk in Chongqing, China: A new identification method and proposal of planning response framework. *Ecological Indicators*, 153. <https://doi.org/10.1016/j.ecolind.2023.110449>
- Iaria, J., & Susca, T. (2022). Analytic Hierarchy Processes (AHP) evaluation of green roof- and green wall-based UHI mitigation strategies via ENVI-met simulations. *Urban Climate*, 46. <https://doi.org/10.1016/j.ulclim.2022.101293>
- Ikaheimo, T. M., Jokelainen, J., Nayha, S., Laatikainen, T., Jousilahti, P., Laukkanen, J., & Jaakkola, J. J. K. (2020). Cold weather-related cardiorespiratory symptoms predict higher morbidity and mortality. *Environmental Research*, 191, Article 110108. <https://doi.org/10.1016/j.envres.2020.110108>
- Ishtiaque, A., Estoque, R. C., Eakin, H., Parajuli, J., & Rabby, Y. W. (2022). IPCC's current conceptualization of 'vulnerability' needs more clarification for climate change vulnerability assessments. *Journal of Environmental Management*, 303. <https://doi.org/10.1016/j.jenvman.2021.114246>
- Kephart, J. L., Sanchez, B. N., Moore, J., Schinasi, L. H., Bakhtsiyarava, M., Ju, Y., Gouveia, N., Caiaffa, W. T., Dronova, I., Arunachalam, S., Diez Roux, A. V., & Rodriguez, D. A. (2022). City-level impact of extreme temperatures and mortality in Latin America. *Nature Medicine*, 28, 1700–1705. <https://doi.org/10.1038/s41591-022-01872-6>
- Klein, T., & Anderegg, W. R. L. (2021). A vast increase in heat exposure in the 21st century is driven by global warming and urban population growth. *Sustainable Cities and Society*, 73. <https://doi.org/10.1016/j.scs.2021.103098>
- Kong, F., Yin, H., James, P., Hutyra, L. R., & He, H. S. (2014). Effects of spatial pattern of greenspace on urban cooling in a large metropolitan area of eastern China. *Landscape and Urban Planning*, 128, 35–47. <https://doi.org/10.1016/j.landurbplan.2014.04.018>
- Lan, T., Peng, J., Liu, Y., Zhao, Y., Dong, J., Jiang, S., Cheng, X., & Corcoran, J. (2023). The future of China's urban heat island effects: A machine learning based scenario analysis on climatic-socioeconomic policies. *Urban Climate*, 49. <https://doi.org/10.1016/j.ulclim.2023.101463>
- Li, M., Zhou, B.-B., Gao, M., Chen, Y., Hao, M., Hu, G., & Li, X. (2022). Spatiotemporal dynamics of global population and heat exposure (2020–2100): Based on improved SSP-consistent population projections. *Environmental Research Letters*, 17. <https://doi.org/10.1088/1748-9326/ac8755>
- Li, X. (2021). Investigating the spatial distribution of resident's outdoor heat exposure across neighborhoods of Philadelphia, Pennsylvania using urban microclimate modeling. *Sustainable Cities and Society*, 72. <https://doi.org/10.1016/j.scs.2021.103066>
- Li, Y., Schubert, S., Kropp, J. P., & Rybski, D. (2020). On the influence of density and morphology on the Urban Heat Island intensity. *Nature Communications*, 11, 2647. <https://doi.org/10.1038/s41467-020-16461-9>
- Liu, H., Huang, B., Zhan, Q., Gao, S., Li, R., & Fan, Z. (2021). The influence of urban form on surface urban heat island and its planning implications: Evidence from 1288 urban clusters in China. *Sustainable Cities and Society*, 71. <https://doi.org/10.1016/j.scs.2021.102987>
- Liu, J., Varghese, B. M., Hansen, A., Zhang, Y., Driscoll, T., Morgan, G., Dear, K., Gourley, M., Capon, A., & Bi, P. (2022). Heat exposure and cardiovascular health outcomes: A systematic review and meta-analysis. *The Lancet Planetary Health*, 6, e484–e495. [https://doi.org/10.1016/S2542-5196\(22\)00117-6](https://doi.org/10.1016/S2542-5196(22)00117-6)
- Ma, L., Huang, G., Johnson, B. A., Chen, Z., Li, M., Yan, Z., Zhan, W., Lu, H., He, W., & Lian, D. (2023). Investigating urban heat-related health risks based on local climate zones: A case study of Changzhou in China. *Sustainable Cities and Society*, 91. <https://doi.org/10.1016/j.scs.2023.104402>
- Martilli, A., Krayenhoff, E. S., & Nazarian, N. (2020). Is the urban heat island intensity relevant for heat mitigation studies? *Urban Climate*, 31. <https://doi.org/10.1016/j.ulclim.2019.100541>
- Massaro, E., Schifanella, R., Piccardo, M., Caporaso, L., Taubenbock, H., Cescatti, A., & Duveiller, G. (2023). Spatially-optimized urban greening for reduction of population exposure to land surface temperature extremes. *Nature Communications*, 14, 2903. <https://doi.org/10.1038/s41467-023-38596-1>
- McElroy, S., Schwarz, L., Green, H., Corcos, I., Guirguis, K., Gershunov, A., & Benmarhnia, T. (2020). Defining heat waves and extreme heat events using sub-regional meteorological data to maximize benefits of early warning systems to population health. *The Science of the Total Environment*, 721, Article 137678. <https://doi.org/10.1016/j.scitotenv.2020.137678>
- Minor, K., Bjerre-Nielsen, A., Jonasdottir, S. S., Lehmann, S., & Obradovich, N. (2022). Rising temperatures erode human sleep globally. *One Earth*, 5, 534–549. <https://doi.org/10.1016/j.oneear.2022.04.008>
- O'Lenick, C. R., Wilhelmi, O. V., Michael, R., Hayden, M. H., Baniassadi, A., Wiedinmyer, C., Monaghan, A. J., Crank, P. J., & Sailor, D. J. (2019). Urban heat and air pollution: A framework for integrating population vulnerability and indoor exposure in health risk analyses. *The Science of the Total Environment*, 660, 715–723. <https://doi.org/10.1016/j.scitotenv.2019.01.002>
- Oke, T., Mills, G., Christen, A., & Voogt, J. (2017). *Urban Climates*. Cambridge University Press.
- Ouyang, Z., Sciusco, P., Jiao, T., Feron, S., Lei, C., Li, F., John, R., Fan, P., Li, X., Williams, C. A., Chen, G., Wang, C., & Chen, J. (2022). Albedo changes caused by future urbanization contribute to global warming. *Nature communications*, 13, 3800. <https://doi.org/10.1038/s41467-022-31558-z>
- Pei, N., Wang, C., Sun, R., Xu, X., He, Q., Shi, X., Gu, L., Jin, J., Liao, J., Li, J., Zhang, L., Zhang, Z., Hao, Z., Jia, B., Qiu, E., Zhang, C., Sun, Z., Jiang, S., Duan, W., Zhang, Y., Zhu, Y., Lepczyk, C. A., Kress, W. J., & Konijnendijk van den Bosch, C. C. (2019). Towards an integrated research approach for urban forestry: The case of China. *Urban Forestry & Urban Greening*, 46. <https://doi.org/10.1016/j.ufug.2019.126472>
- Psistaki, K., Dokas, I. M., & Paschalidou, A. K. (2023). Analysis of the heat- and cold-related cardiovascular mortality in an urban mediterranean environment through various thermal indices. *Environmental Research*, 216, Article 114831. <https://doi.org/10.1016/j.envres.2022.114831>
- Ren, Z., Fu, Y., Dong, Y., Zhang, P., & He, X. (2022). Rapid urbanization and climate change significantly contribute to worsening urban human thermal comfort: A national 183-city, 26-year study in China. *Urban Climate*, 43. <https://doi.org/10.1016/j.ulclim.2022.101154>
- Ruiz-Paez, R., Diaz, J., Lopez-Bueno, J. A., Navas, M. A., Miron, I. J., Martinez, G. S., Luna, M. Y., & Linares, C. (2023). Does the meteorological origin of heat waves

- influence their impact on health? A 6-year morbidity and mortality study in Madrid (Spain). *The Science of the total environment*, 855, Article 158900. <https://doi.org/10.1016/j.scitotenv.2022.158900>
- Sadeghi, M., de Dear, R., Morgan, G., Santamouris, M., & Jalaludin, B. (2021). Development of a heat stress exposure metric – Impact of intensity and duration of exposure to heat on physiological thermal regulation. *Building and Environment*, 200.
- Sherwood, S. C., & Huber, M. (2010). An adaptability limit to climate change due to heat stress. *Proceedings of the National Academy of Sciences of the United States of America*, 107, 9552–9555. <https://doi.org/10.1016/j.buildenv.2021.107947>
- Siddiqui, A., Kushwaha, G., Nikam, B., Srivastav, S. K., Shelar, A., & Kumar, P. (2021). Analysing the day/night seasonal and annual changes and trends in land surface temperature and surface urban heat island intensity (SUHII) for Indian cities. *Sustainable Cities and Society*, 75. <https://doi.org/10.1016/j.scs.2021.103374>
- Sun, L., Chen, J., Li, Q., & Huang, D. (2020). Dramatic uneven urbanization of large cities throughout the world in recent decades. *Nature communications*, 11, 5366. <https://doi.org/10.1038/s41467-020-19158-1>
- Sun, Y., Zhang, C., Zhao, Y., Li, J., Ma, Y., & Zhu, C. (2023). A systematic review on thermal environment and thermal comfort studies in Chinese residential buildings. *Energy and Buildings*, 291. <https://doi.org/10.1016/j.enbuild.2023.113134>
- Tian, P., Li, J., Cao, L., Pu, R., Wang, Z., Zhang, H., Chen, H., & Gong, H. (2021). Assessing spatiotemporal characteristics of urban heat islands from the perspective of an urban expansion and green infrastructure. *Sustainable Cities and Society*, 74. <https://doi.org/10.1016/j.scs.2021.103208>
- Ullah, S., You, Q., Chen, D., Sachindra, D. A., Aghakouchak, A., Kang, S., Li, M., Zhai, P., & Ullah, W. (2022). Future population exposure to daytime and nighttime heat waves in South Asia. *Earth's Future*, 10. <https://doi.org/10.1029/2021EF002511>
- Wang, C., Ren, Z., Dong, Y., Zhang, P., Guo, Y., Wang, W., & Bao, G. (2022a). Efficient cooling of cities at global scale using urban green space to mitigate urban heat island effects in different climatic regions. *Urban Forestry & Urban Greening*, 74. <https://doi.org/10.1016/j.ufug.2022.127635>
- Wang, C., Ren, Z., Du, Y., Guo, Y., Zhang, P., Wang, G., Hong, S., Ma, Z., Hong, W., & Li, T. (2023a). Urban vegetation cooling capacity was enhanced under rapid urbanization in China. *Journal of Cleaner Production*. <https://doi.org/10.1016/j.jclepro.2023.138906>
- Wang, J., Chen, Y., Liao, W., He, G., Tett, S. F. B., Yan, Z., Zhai, P., Feng, J., Ma, W., Huang, C., & Hu, Y. (2021). Anthropogenic emissions and urbanization increase risk of compound hot extremes in cities. *Nature Climate Change*. <https://doi.org/10.1038/s41558-021-01196-2>
- Wang, J., McPhearson, T., Zhou, W., Cook, E. M., Herreros-Cantis, P., & Liu, J. (2023b). Comparing relationships between urban heat exposure, ecological structure, and socio-economic patterns in Beijing and New York City. *Landscape and Urban Planning*, 235. <https://doi.org/10.1016/j.landurbplan.2023.104750>
- Wang, J., Zhou, W., & Jiao, M. (2022b). Location matters: Planting urban trees in the right places improves cooling. *Frontiers in Ecology and the Environment*, 20, 147–151. <https://doi.org/10.1002/fee.2455>
- Wang, Y., Wang, A., Zhai, J., Tao, H., Jiang, T., Su, B., Yang, J., Wang, G., Liu, Q., Gao, C., Kundzewicz, Z. W., Zhan, M., Feng, Z., & Fischer, T. (2019). Tens of thousands additional deaths annually in cities of China between 1.5 degrees C and 2.0 degrees C warming. *Nature Communications*, 10, 3376. <https://doi.org/10.1038/s41467-019-11283-w>
- Wu, W., Chen, W. Y., Yun, Y., Wang, F., & Gong, Z. (2022). Urban greenness, mixed land-use, and life satisfaction: Evidence from residential locations and workplace settings in Beijing. *Landscape and Urban Planning*, 224. <https://doi.org/10.1016/j.landurbplan.2022.104428>
- Wu, X., & Tang, S. (2022). Comprehensive evaluation of ecological vulnerability based on the AHP-CV method and SOM model: A case study of Badong County, China. *Ecological Indicators*, 137. <https://doi.org/10.1016/j.ecolind.2022.108758>
- Yuan, B., Zhou, L., Hu, F., & Zhang, Q. (2022). Diurnal dynamics of heat exposure in Xi'an: A perspective from local climate zone. *Building and Environment*, 222. <https://doi.org/10.1016/j.buildenv.2022.109400>
- Zhao, L., Lee, X., Smith, R. B., & Oleson, K. (2014). Strong contributions of local background climate to urban heat islands. *Nature*, 511, 216–219. <https://doi.org/10.1038/nature13462>
- Zhi, G., Meng, B., Wang, J., Chen, S., Tian, B., Ji, H., Yang, T., Wang, B., & Liu, J. (2021). Spatial analysis of urban residential sensitivity to heatwave events: Case studies in five megacities in China. *Remote Sensing*, 13. <https://doi.org/10.3390/rs13204086>
- Zhou, D., Bonafoni, S., Zhang, L., & Wang, R. (2018). Remote sensing of the urban heat island effect in a highly populated urban agglomeration area in East China. *Science of the Total Environment*, 628–629, 415–429. <https://doi.org/10.1016/j.scitotenv.2018.02.074>
- Zhou, W., Huang, G., Pickett, S. T. A., Wang, J., Cadenasso, M. L., McPhearson, T., Grove, J. M., & Wang, J. (2021). Urban tree canopy has greater cooling effects in socially vulnerable communities in the US. *One Earth*, 4, 1764–1775. <https://doi.org/10.1016/j.oneear.2021.11.010>
- Zhou, Y., Zhao, H., Mao, S., Zhang, G., Jin, Y., Luo, Y., Huo, W., Pan, Z., An, P., & Lun, F. (2022). Studies on urban park cooling effects and their driving factors in China: Considering 276 cities under different climate zones. *Building and Environment*, 222. <https://doi.org/10.1016/j.buildenv.2022.109441>
- Zhu, W., & Yuan, C. (2023). Urban heat health risk assessment in Singapore to support resilient urban design — By integrating urban heat and the distribution of the elderly population. *Cities*, 132. <https://doi.org/10.1016/j.cities.2022.104103>